

Generation of a humanized afucosylated BAFF-R antibody with broad activity against human B-cell malignancies

Zhenyuan Dong,¹ Joo Y. Song,² Elana Thieme,¹ Aaron Anderson,¹ Elizabeth Oh,¹ Wesley A. Cheng,¹ Benjamin Z. Kuang,¹ Vincent Lee,¹ Tiantian Zhang,¹ Zhe Wang,¹ Szymon Szymura,¹ D. Lynne Smith,³ Jianbing Zhang,⁴ Weihong Nian,⁵ Xintong Zheng,⁵ Feng He,⁵ Qing Zhou,⁵ Soung-chul Cha,¹ Alexey V. Danilov,¹ Hong Qin,¹ and Larry W. Kwak¹

¹Toni Stephenson Lymphoma Center, Department of Hematology and Hematopoietic Stem Cell Transplantation, Beckman Research Institute of City of Hope, Duarte, CA; ²Department of Pathology, City of Hope Medical Center, Duarte, CA; ³Clinical and Translational Project Development, City of Hope Medical Center, Duarte, CA; ⁴Innolifex Inc., Palo Alto, CA; and ⁵Shanghai Escugen Biotechnology Co, Ltd, Shanghai, China

Key Points

- BAFF-R survival receptor is an attractive therapeutic target because it is critically involved in B-cell lymphoma/leukemia survival
- Humanized BAFF-R antibody was optimized for ADCC and has antitumor activity in patient-derived and human lymphoma/leukemia xenograft models

B-cell activating factor receptor (BAFF-R) is a mature B-cell survival receptor, which is highly expressed in a wide variety of B-cell malignancies but with minimal expression in immature B cells. These properties make BAFF-R an attractive target for therapy of B-cell lymphomas. We generated a novel humanized anti BAFF-R monoclonal antibody (mAb) with high specificity and potent *in vitro* and *in vivo* activity against B-cell lymphomas and leukemias. The humanized variants of an original chimeric BAFF-R mAb retained BAFF-R binding affinity and antibody-dependent cellular cytotoxicity (ADCC) against a panel of human cell lines and primary lymphoma samples. Furthermore, 1 humanized BAFF-R mAb clone and its afucosylated version, glycoengineered to optimize the primary mechanism of action, prolonged survival of immunodeficient mice bearing human tumor cell lines or patient-derived lymphoma xenografts in 3 separate models, compared with controls. Finally, the tissue specificity of this humanized mAb was confirmed against a broad panel of normal human tissues. Taken together, we have identified a robust lead-candidate BAFF-R mAb for clinical development.

Introduction

Therapeutic monoclonal antibodies (mAbs) have been used widely and successfully in hematologic malignancies, which began with the approval of the anti-CD20 rituximab in 1997.¹ The B-lymphocyte lineage-specific surface antigens CD20 and CD19 have been the targets of clinically relevant mAbs for lymphomas and leukemias, which, however, still remain incurable because of emerging resistance. In B-cell malignancies, for example, resistance to rituximab is caused by multiple mechanisms including the downregulation of CD20 expression upon repeated exposure.² There is clearly a need for the development of mAbs to alternative therapeutic targets in resistant B-cell malignancies.

The tumor necrosis factor receptor superfamily member, B-cell activating factor receptor (BAFF-R/TNFRSF13C), is 1 such target.^{3,4} BAFF-R is a particularly attractive target because it is specifically involved in B-lymphocyte development and is expressed almost exclusively on B cells, including all subtypes of mature human B-cell lymphomas.⁵ The BAFF/BAFF-R axis has been successfully targeted

Submitted 14 July 2022; accepted 11 November 2022; prepublished online on *Blood Advances* First Edition 5 December 2022; final version published online 16 March 2023. <https://doi.org/10.1182/bloodadvances.2022008560>.

Data and materials produced in this study are protected by City of Hope intellectual property patents but will remain available to qualified investigators at other research organization by establishing a Material Transfer Agreement (MTA). MTA requests should be directed to the corresponding author, Larry W. Kwak (lkwak@coh.org).

The full-text version of this article contains a data supplement.

© 2023 by The American Society of Hematology. Licensed under [Creative Commons Attribution-NonCommercial-NoDerivatives 4.0 International \(CC BY-NC-ND 4.0\)](https://creativecommons.org/licenses/by-nc-nd/4.0/), permitting only noncommercial, nonderivative use with attribution. All other rights reserved.

for the treatment of autoimmune diseases, particularly with mAbs directed against the BAFF ligand.⁶ In addition to our previous report of a chimeric BAFF-R mAb (C90) with activity in models of drug-resistant mantle cell lymphoma (MCL),⁷ another anti-BAFF-R mAb was effective at reducing murine B-cell populations in vivo but no data on activity against malignant B cells were provided,⁸ and a fully human anti-BAFF-R Ab (B-1239/VAY736/ianalumab) has shown some activity in models of Philadelphia-positive pre-B acute lymphoblastic leukemia (ALL)⁹ and chronic lymphocytic leukemia/lymphoma (CLL).^{10,11} Ianalumab is now in early clinical development in combination with ibrutinib in patients with CLL.^{12,13}

Clearly, anti-BAFF-R mAbs show promising signs of therapeutic potential in B-cell malignancies. To further develop our BAFF-R mAb for clinical application, we humanized our original chimeric Ab (C90),⁷ to reduce potential immunogenicity.¹⁴ In this report we describe the generation, in vitro and in vivo optimization of humanized variants of C90, and the identification of a lead-candidate humanized anti-BAFF-R mAb with appropriate specificity.

Methods

Animals, cell lines, and primary human tumor samples

Mice. Nonobese diabetic/severe combined immunodeficiency/ γ Cnull (NOD.Cg-Prkdc^{scid} Il2rg^{tm1Wjl}/SzJ [NSG]) mice were either purchased directly as 8-week-old individuals or as breeding pairs from The Jackson Laboratory (Bar Harbor, ME) to maintain an NSG breeding colony at the Animal Resource Center at City of Hope. Mice were housed in a pathogen-free animal facility according to institutional guidelines. All animal studies were approved by the Institutional Animal Care and Use Committee (IACUC #15020).

Tumor and cell lines. Commercially available tumor cell lines Raji, RL, JeKo-1, Z-138, and Nalm6 were purchased from the American Type Culture Collection (ATCC) (Manassas, VA). RS4;11, MEC-1, and HL-60 were obtained from The Leibniz Institute German Collection of Microorganisms and Cell Cultures (Brunswick, Germany). Human natural killer (NK)-92 176V cells were obtained from CONKWEST Life Sciences Company (San Diego, CA). Ly-10 cell line was provided by Marcin Kortylewski of the Beckman Research Institute of the City of Hope. MCL96069 (*BIRC3*^{L548fs}) patient-derived xenografts (PDXs) were obtained from the Public Repository of Xenografts (ProXe; www.proxe.org).¹⁵

Human blood and tumor samples. Noncultured, primary human lymphomas were obtained from the lymphoma satellite tissue bank at MD Anderson Cancer Center under an Institutional Review Board (IRB)-approved protocol (protocol, 2005-0656). Primary patient samples included leukapheresis or blood from patients with MCL or CLL, and excised lymph nodes from patients with diffuse large B-cell lymphoma (DLBCL) or follicular lymphoma (FL). Samples were cryopreserved as viable single-cell suspensions in 10% dimethyl sulfoxide without additional enrichment or sorting. The percentage of tumor cells in each sample ranged from 80% to 98% for leukapheresis or blood, and from 50% to 60% for lymph node biopsies. Normal donor peripheral blood mononuclear cells (PBMC) for NK-cell isolation was provided by the Michael

Amini Transfusion Medicine Center at City of Hope under an IRB-approved protocol (protocol, 15283).

Humanized BAFF-R Abs

LakePharma (San Carlos, CA) was contracted to produce 3 light chain (VL) and 3 heavy-chain (VH) variants of our previously described BAFF-R chimeric C90 mAb (C90)⁷ to produce 9 humanized Ab variants. For each of the 9 VL/VH combination antibodies, Lake Pharma provided expression plasmids, humaneness scores, and dissociation constants (K_D). K_Ds were determined by surface plasmon resonance and were a measure of the strength of attraction between receptor (BAFF-R Ab) and ligand (BAFF-R). K_D is calculated by the off-rate (k_{off}) divided by the on-rate (k_{on}): $K_D = \frac{k_{off}}{k_{on}}$.

Generation, production, and purification of humanized Abs

To enable head-to-head comparisons in the functional studies, all Ab variable regions were cloned into pFUSEss-CHlg-hG1e4 and pFUSE2ss-CLlg-hk (InvivoGen, San Diego, CA) to produce heavy-chain and light-chain immunoglobulin G1 (IgG1) peptides, respectively. All humanized versions of BAFF-R C90⁷ were produced by polymerase chain reaction amplification of heavy and light chain variable region sequences provided as VH1, VH2, VH3, VL1, VL2, and VL3 in the pcDNA3.1 vector backbone by Lake Pharma. Heavy- and light-chain vectors were cotransfected at a 1:2 ratio into Freestyle 293-F cells (Expi293F) (Life Technologies, Carlsbad, CA) grown in Freestyle 293 expression medium (Life Technologies) in a 37°C, humidified, 8% CO₂ incubator with 120-RPM shaking. For the transfection, 2 mL of 500 µg/mL polyethylenimine MAX (Polysciences, Inc, Warrington, PA) were mixed with 2 mL of 100 µg/mL total plasmid DNA, which was then added to 2 × 10⁸ cells in 100 mL medium after which cells were cultured for 6 days before harvesting. Antibody-containing supernatant was collected and diluted 1:5 with phosphate-buffered saline (PBS). The Abs were purified by protein-A affinity chromatography according to the manufacturer's directions (GE Healthcare, Marlborough, MA) and stored in PBS. All Abs were assessed for purity by sodium dodecyl sulfate–polyacrylamide gel electrophoresis, for affinity by enzyme-linked immunosorbent assay (ELISA), and activity by Ab-dependent cellular cytotoxicity (ADCC), as described in further sections.

Generation of afucosylated H90

Afucosylated H90-5 (H90-AF), a glycosylated IgG1-κ, was produced in Chinese hamster ovary (CHO)-DG44 cells, stably transfected with the pAB11_DHFR_Dual expression vector (Aragen Bioscience Inc, Morgan Hill, CA) containing the complementary DNA (cDNA) sequences of the humanized light- and heavy-chain variable regions, and the human constant region of H90-5. Cells were grown in a 14-day feed-batch suspension culture in Escugen Biotechnology Co Ltd proprietary chemically defined medium in a 15-L bioreactor. Growth medium was supplemented with a proprietary fucosyltransferase inhibitor to reduce Ab core fucosylation. The culture medium was harvested by depth filtration and Ab purified using protein-A affinity chromatography, low-pH virus inactivation, and anion exchange and cation exchange chromatography. Afucosylation of H90-5 was verified by analysis of Ab

oligosaccharide components using hydrophilic interaction liquid chromatography (HILIC), coupled with mass spectrometry.

ELISA for BAFF-R Ab binding

The ELISA was performed with recombinant human BAFF receptor-coated (PeproTech, Cranbury, NJ) micro-well plates with twofold serial dilutions of test Abs (C90; or H90-1 through H90-9) incubated at room temperature for 1 hour. Secondary Ab goat antihuman IgG-HRP (Thermo Fisher, Waltham, MA) was diluted according to the manufacturer's recommendation and incubated for 1 hour at room temperature. Wells were incubated with Step Ultra TMB-ELISA substrate solution (Thermo Fisher) for 10 minutes followed by 2N sulfuric acid quench. Samples were read at an optical density of 450 nm on a SpectraMax Plus 384 micro plate reader (Molecular Devices, San Jose, CA).

Flow cytometry and cell sorting

The recombinant Abs were labeled for characterization of their binding specificity using flow cytometry analysis. Biotinylated H90-4 and H90-5 (100 ng) per 10^6 target cell-bound cells were detected using Abs labeled with phycoerythrin (PE)-labeled streptavidin alongside commercial fluorescently labeled Abs against other cell surface markers to stain target cells.

All flow cytometry procedures were performed on a BD LSR Fortessa (Becton Dickinson, Franklin Lakes, NJ). Staining procedures were performed using staining buffer (fetal bovine serum [FBS]) (RUO) (Becton Dickinson). Data were analyzed using FlowJo software (FlowJo, LLC, Ashland, OR).

Antibody binding to BAFF-R variants

To generate common BAFF-R variants, BAFF-R wild-type (WT), p21R variant, or G64V variant cDNA together with T2A self-cleaving peptide were cloned into a pcDNA-green fluorescent protein (GFP) vector (Plasmid #160697; Addgene) under the cytomegalovirus promoter. Then, 293T cells were cultured in 10 cm plates to express each variant using transfection protocols with 17 μ g of plasmid and 51 μ L of FuGENE 6 transfection reagent. Resulting cells were harvested 48 hours after transfection. Cells were then stained with H90-4 and H90-5 at doses ranging between 0.01 ng and 10 ng per 10^6 cells. For detection, cells were stained with the Allophycocyanin (APC)-labeled goat antihuman secondary Ab. An APC-labeled antihuman BAFF-R mAb (11C1) was used as a positive control and analyzed as described earlier. Staining procedures were performed using staining buffer (FBS) (RUO) (Becton Dickinson).

Cytotoxicity assays

Target cells (2×10^6) (BAFF-R-expressing human tumor cell lines, primary patient-derived tumor samples) were incubated with 100 μ L chromium-51 (^{51}Cr) solution (1 $\mu\text{Ci}/\text{mL}$; Perkin Elmer, Waltham, MA) for 1 hour at 37°C in a humidified 5% CO_2 incubator. After removing excess ^{51}Cr , cells were resuspended in 10 mL of RPMI-1640 glutaMAX media (Life Technologies) with 10% (v/v) FBS (Omega Scientific, Tarzana, CA) to a final concentration of 2×10^5 cells per mL. Cells (50 μ L) were combined with 50 μ L of Ab prepared in RPMI-1640 glutaMAX media (Life Technologies) with 10% (v/v) FBS at test concentrations (5 $\mu\text{g}/\text{mL}$) (Figure 1C,E) or serial dilutions (10^{-6} $\mu\text{g}/\text{mL}$ to 10 $\mu\text{g}/\text{mL}$) of this Ab preparation, as indicated in Figure 2D. Effector NK cells were isolated from donor

PBMC with a human NK-cell enrichment kit (Stemcell Technologies, Inc, Vancouver, BC, Canada) and resuspended in RPMI-1640 glutaMAX media (Life Technologies) with 10% (v/v) FBS to the appropriate effector-to-target (E:T) concentrations. Effector cells (50 μ L) were added to the appropriate experimental groups. Cells were mixed well and maintained for either 6 hours or overnight, at 37°C in a humidified 5% CO_2 incubator. At the end of the incubation period, ^{51}Cr released into the supernatant was analyzed by sampling clarified supernatant and detecting radioactivity with a gamma counter (Wallac Wizard 1470 Automatic Gamma Counter, Perkin Elmer). Percent lysis was calculated using the equation: $\text{lysis} (\%) = -\frac{\text{CPM} - \text{SR}}{\text{MR} - \text{SR}} \times 100\%$ | SR: CPM of spontaneous release; MR: CPM of maximum release. For comparison of H90-5 and H90-AF the target cells were of human B-lymphoblast cell line RL with engineered NK-92MI-CD16a effector cells (provided by Escugen Biotechnology). The target cells were suspended in RPMI-1640 (Thermo Fisher, Waltham, MA) with 5% (v/v) FBS to a density of 2×10^5 cells per mL. Effector cells were suspended in the same medium to 1×10^6 cells per mL. The target and effector cell suspensions (50 μ L each) were mixed in the wells of a 96-U cell culture plate. H90-5, H90-AF, and rituximab were prepared with the cell culture medium at 1 $\mu\text{g}/\text{mL}$, and with 10-fold serial dilutions. An irrelevant IgG1 isotype control (Escugen, Shanghai, China) was also prepared in parallel as a negative-control reagent. Ab dilutions (100 μ L) were mixed with the cells and incubated in 96-well plates for 4 hours at 37°C in a humidified 5% CO_2 incubator. Supernatants were collected and lactate dehydrogenase release was measured using the CytoTox 96 nonradioactive cytotoxicity assay kit (Promega, Madison, WI) with a 96-well plate reader. Percent cytotoxicity was calculated using the equation: $\% \text{ cytotoxicity} (\%) = (\text{experimental release} - \text{effector cell spontaneous release} - \text{target spontaneous release}) / (\text{target maximum release} - \text{target spontaneous release}) \times 100\%$.

Antibody glycan profile analysis

N-linked oligosaccharides were cleaved off from the Ab with N-glycosidase. The oligosaccharide component was analyzed using HILIC, coupled with mass spectrometry. Abs H90-5 or H90-AF (200 μg each) were dissolved in 180 μ L of 50 mM phosphate buffer, and 20 μ L of 10 \times denaturing buffer (New England Biolabs, Woburn, MA). The Abs were denatured by heating at 100°C for 10 minutes. N-linked oligosaccharides were cleaved by N-glycosidase F by adding 40 μ L of 10% NP-40 and 1 μ L of PNGaseF (New England Biolabs), followed by incubation at 37°C for ~16 to 24 hours. The cleavage reaction was stopped with 500 μ L of pre-cooled ethanol and subsequent freezing at -80°C for 30 minutes. The aqueous layer of 500 μ L was collected by centrifugation for 13 000 rpm for 10 minutes, followed by centrifugal evaporation. The products were dissolved in 10 μ L of water with 10 μ L of the labeling reagent solution (50 mg, 2-aminobenzamide; 60 mg sodium cyanotrihydridoborate in 300 μ L of glacial acetic acid; and 700 μ L dimethyl sulfoxide) at 65°C for 2.5 hours. The sample was mixed with 80 μ L of 70% acetonitrile (ACN) at room temperature until all sediment was dissolved. The aqueous layer was collected for analysis using HILIC. HILIC-ultra-performance liquid chromatography (UPLC) analysis was performed on a Waters ACQUITY UPLC H-Class system equipped with a fluorescence detector ($\lambda_{\text{ex}} = 330\text{nm}$; $\lambda_{\text{em}} = 420\text{nm}$) using a glycan BEH amide column (2.1 \times 150 mm, 1.7 μm ; Waters Corporation, Milford, MA) and gradient elution (phase A, 50 mM

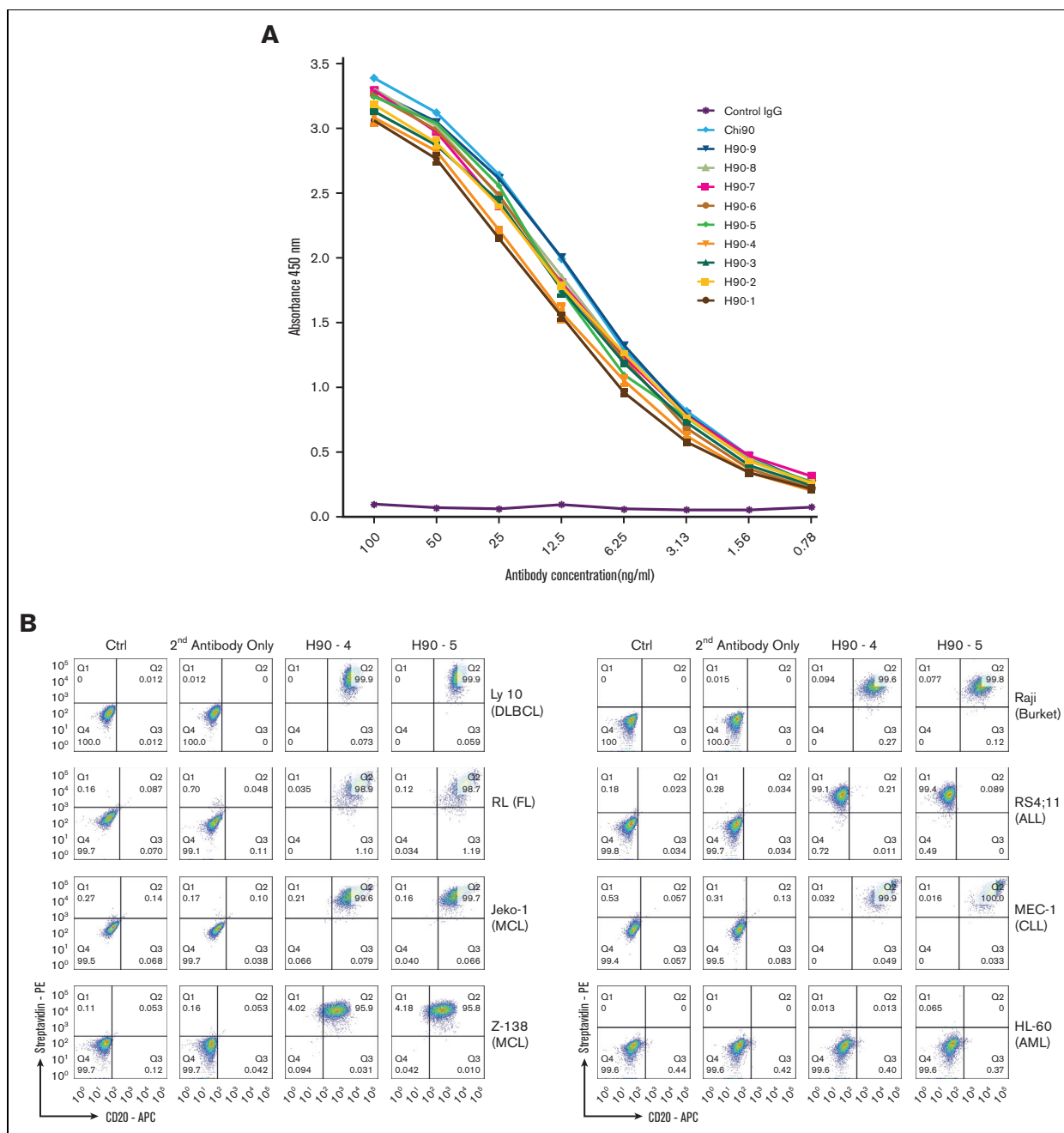


Figure 1. In vitro characterization of humanized anti-BAFF-R mAbs. (A) Binding affinities of 9 selected humanized Abs derived from the C90 sequence by ELISA, as described in Methods. (B) Specificity of 2 candidates, H90-4 and H90-5, analyzed by flow cytometry staining of human B-cell malignancy lines representative of the following diseases: Burkitt lymphoma (Raji), ALL (RS4;11), CLL (MEC-1), acute myeloid leukemia (HL-60), DLBCL (Ly 10), follicular lymphoma (RL), and MCL (Jeko-1, Z-138). (C) ADCC assays of H90-4 and H90-5 against B-cell lines as indicated. Anti-CD20 mAb rituximab was used as a positive control. Negative controls were human IgG and NK cells alone. Target cell lines were incubated with Abs at 5 $\mu\text{g}/\text{mL}$, and fresh NK cells at E:T ratio of 20:1 for 6 hours. Specific cytotoxicity was calculated as in Methods. Experiments were conducted in triplicate and data were analyzed by Student *t* test. (D) Flow cytometry of H90-4 and H90-5 (100 ng/ 10^6 cells) on human primary tumor samples. (E) H90-4 and H90-5 to 5 ADCC assays against primary patient tumor cells. Target cells were incubated with Abs at 5 $\mu\text{g}/\text{mL}$, and fresh NK cells at E:T ratio of 20:1 for 6 hours. (F) 293T cells were transfected with the BAFF-R wild-type or P21R/G64V variants as described in Methods. Cells were then stained with different amounts of H90-4/H90-5 with a secondary goat antihuman APC or antihuman BAFF-R mAb (11C1) as positive controls. Unstained cells and secondary Ab (antihuman IgG-APC) served as negative controls. Experiments were conducted in triplicate and analyzed by Student *t* test. Data shown are representative of 3 independent experiments. Ctrl, control.

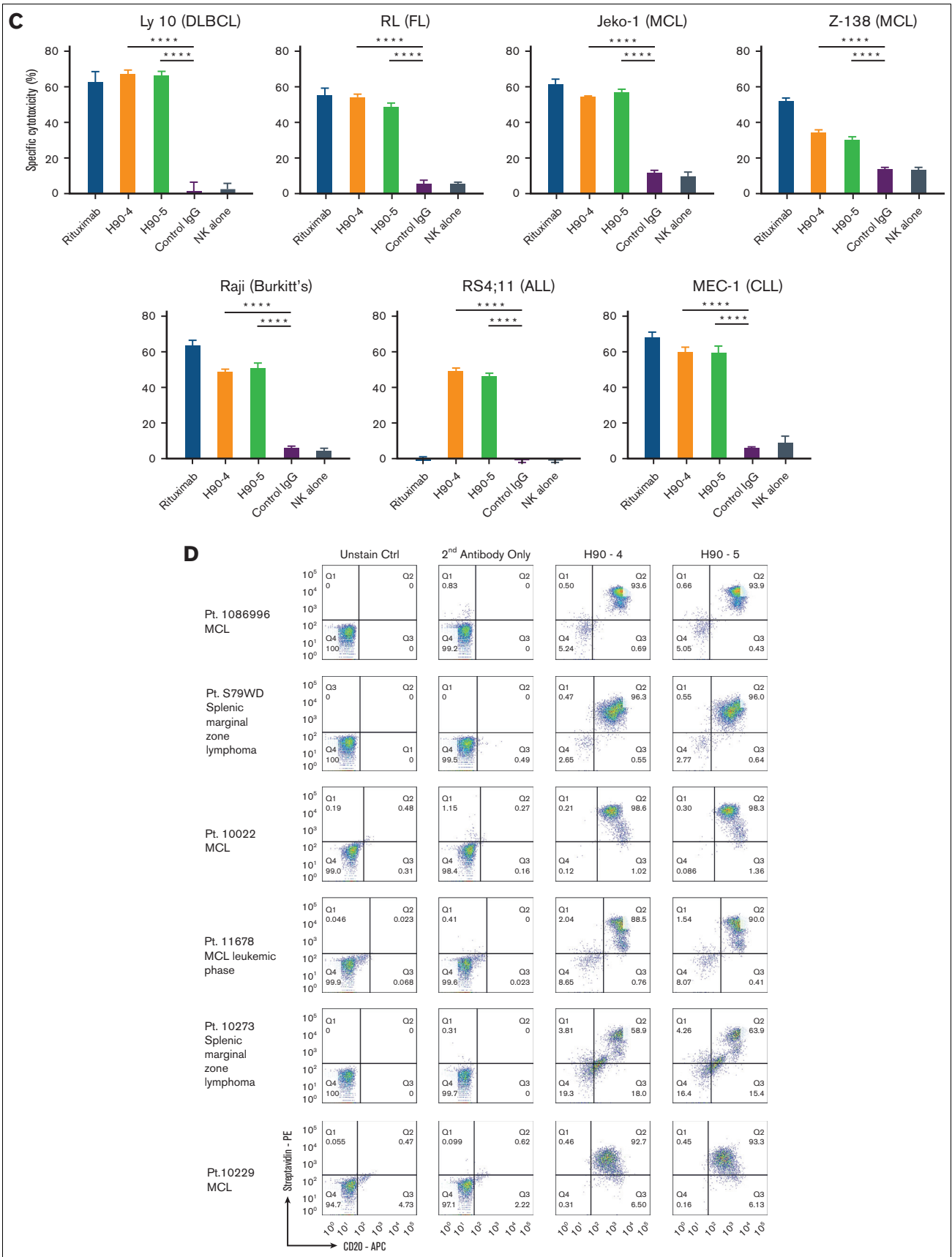


Figure 1 (continued)

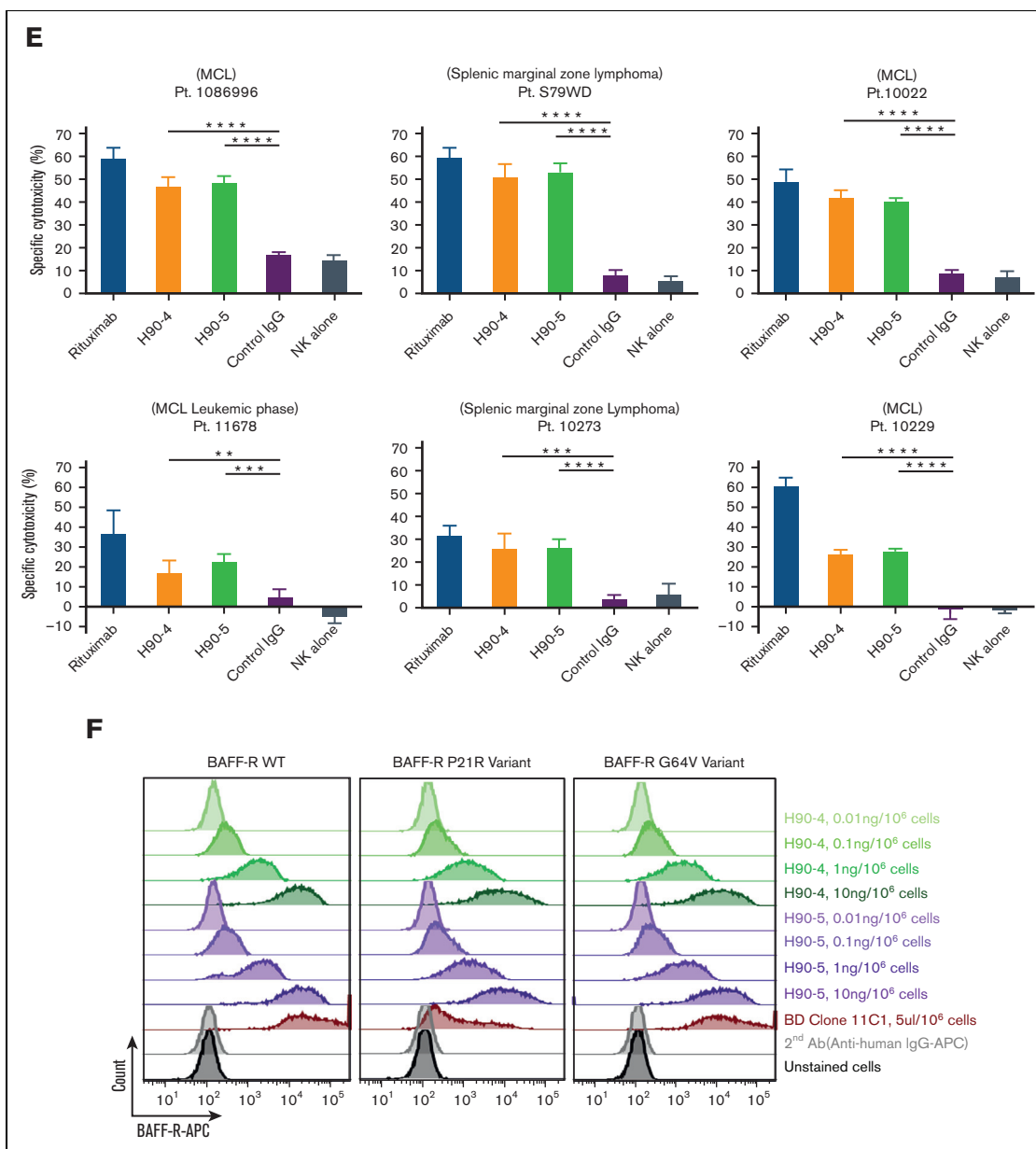


Figure 1 (continued)

ammonium, pH 4.40; phase B, 100% ACN). The sample was eluted with the following gradient: 0 to 5 minutes, 22% phase A at a flow rate of 0.5 mL/min; 5-33 minutes, 22%-40% phase A at a flow rate of 0.5 mL/min; 34-39 minutes, 80% phase A at a flow rate of 0.25 mL/min; column equilibration, 41-50 minutes, with 22% phase A at a flow rate of 0.5 mL/min (column temperature maintained at 60°C). All glycosylation peaks were identified by mass-to-charge ratios on ThermoFisher Q Exactive Orbitrap mass spectrometers (Thermo Fisher Scientific, Waltham, MA).

Antibody mass analysis

Intact mass analysis was performed to characterize N-glycosylation uniformity of H90-AF. Vanquish-F UPLC (Thermo Fisher Scientific)

with a Mab Pac reversed-phase column (4 μ m, 2.1 \times 50 mm; Thermo Fisher Scientific) were used for separation. The column was initially equilibrated in 80% phase A (0.1% formic acid in water) and 20% phase B (0.1% formic acid in ACN) at a flow rate of 0.5 mL/min with a column temperature of 80°C. The 5-minute gradient was programmed as follows: 0 to 0.5 minutes, 20% phase B; 0.5 to 2.5 minutes, 20%-50% phase B; 2.5-3 minutes, 50% phase B; 3 to 3.5 minutes, phase B was increased to 90% and maintained at 90% phase B to 4 minutes; and finally, 4 to 5 minutes, 20% phase B (column reequilibration). The Q Exactive Plus Quadrupole-Orbitrap mass spectrometer (Thermo Fisher Scientific) was used for mass detection in positive mode, with spray voltage set to 3.8 kV and nitrogen as drying gas at a flowrate of 3.5 L/min at 300°C. Data were

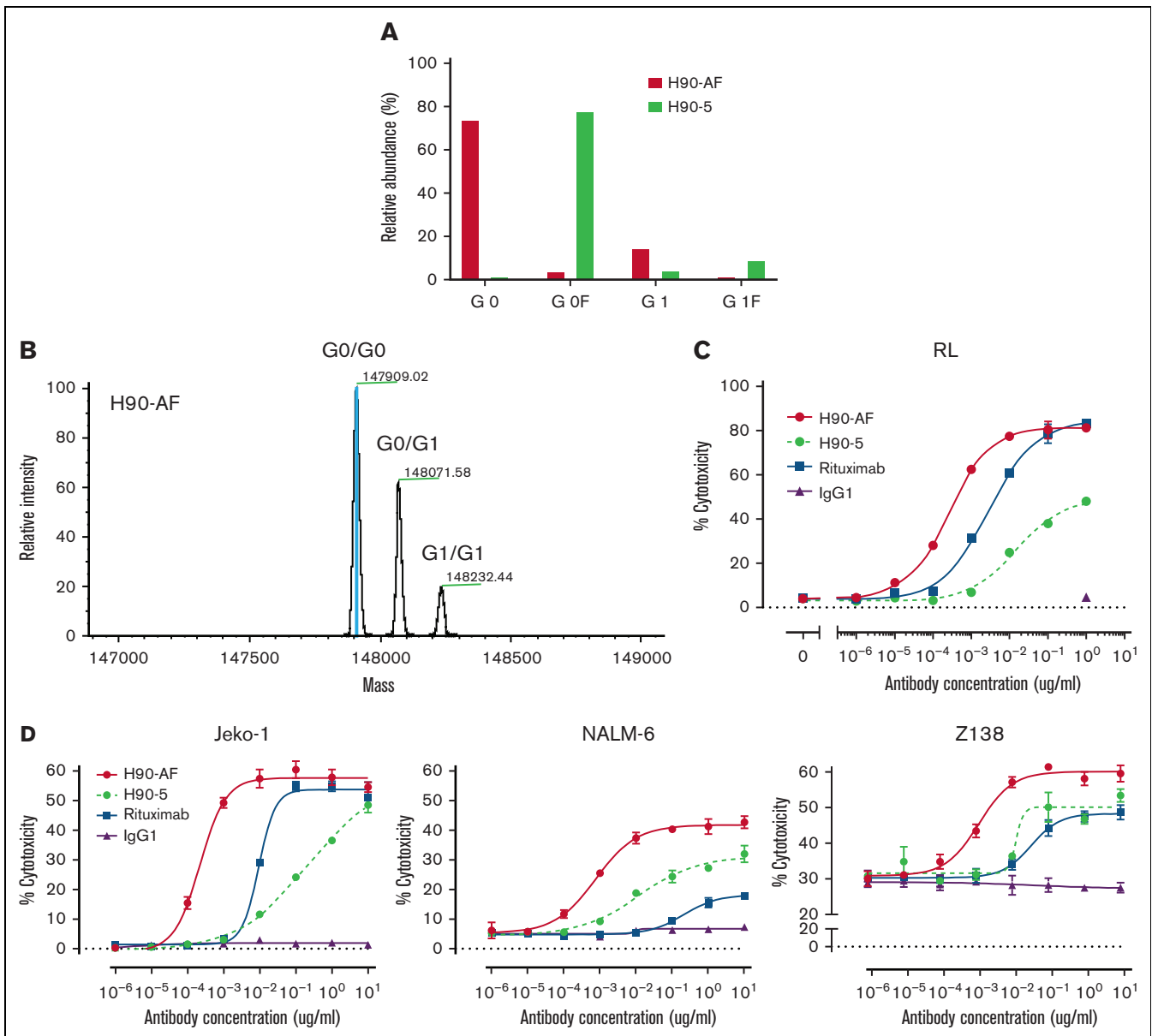


Figure 2. In vitro characterization of anti-BAFF-R afucosylated Ab, H90-AF. (A) Proportions of G0 and G1 core-fucosylated chains derived from H90-5 and H90-AF. The percentage of fucosylation of the oligosaccharide chains from each species of Ab is plotted and compared. (B) Deconvoluted mass spectra of H90-AF. Assigned glycoforms and observed mass are annotated on detected peaks. (C) ADCC assays of H90-5 and H90-AF against RL target cells with NK-92MI-CD16a effector cells at an E:T ratio of 5:1. Rituximab served as a positive control and an irrelevant IgG1 was the negative control. (D) ADCC assays of H90-5 and H90-AF against Jeko-1, Nalm-6, and Z138 target cells with NK cells from PBMC as effector cells at an E:T ratio of 10:1. Experiments were conducted in triplicate.

acquired in the mass-to-charge ratio range of 800 to 4000 and analyzed using BiopharmaFinder software (Thermo Fisher Scientific).

Human lymphoma and leukemia cell line xenograft studies

In vivo studies were carried out with MCL cell line Z-138 and ALL cell line Nalm6. Red luciferase-expressing tumor cells were generated for in vivo imaging of tumor development by stable transduction with lentivirus-expressing red luciferase together with

a GFP reporter (Life Technologies). GFP-positive cells were sorted by flow cytometry and a stable luciferase-expressing lines were expanded.

Functional in vivo studies of selected Abs were performed in NSG mice (Jackson Laboratory). For each experiment, each mouse was challenged with the minimum lethal dose of tumor cells (5×10^4 Z-138; 1.0×10^5 Nalm6) suspended in 300 μ L PBS (day 0). Tumors were allowed to engraft for 3 days before Ab treatments, which occurred on days 3, 7, 11, and 15. Treatments consisted of a 300 μ L IV injection containing 15×10^6 effector human NK-92 176V cells, 1.5×10^6

(Nalm6 xenografts), or 2.0×10^6 (Z-138 xenografts) NK cells enriched from a healthy male donor using a NK-cell enrichment kit (Thermo Fisher), with 300 μg treatment Ab and 5×10^4 IU interleukin 2 (IL-2) (Prometheus Therapeutics & Diagnostics, San Diego, CA). Control groups received the same volume of injection with PBS or NK cells with IL-2. Bioluminescent imaging was performed once or twice a week for up to 50 days. For bioluminescent imaging, mice were anesthetized with isoflurane and administered 150 mg/kg D-luciferin (Life Technologies) via subcutaneous injection 10 minutes before imaging. In vivo bioluminescence imaging was performed on an AmiX imaging system (Spectral Instruments Imaging, Tucson, AZ). Survival was tracked up to 100 days after tumor challenge.

PDXs

Eight-week-old NSG mice received 25 mg/kg busulfan via intraperitoneal injection. After 24 hours, MCL cells from the PDX model MCL96069 (*BIRC3*^{L548fs}) were inoculated via tail vein injection (3×10^6 MCL cells in 200 μL PBS). Three days after tumor challenge, mice received Ab treatments, which occurred on days 3, 7, 11, and 15. Treatments consisted of a 300 μL IV injection containing 300 μg treatment Ab (either H90-5, C90, or H90-AF), 2×10^6 NK cells enriched from a healthy donor as described earlier, and 5×10^4 IU IL-2. Control groups received the same volume of injection with PBS alone or NK cells with IL-2.

Peripheral blood was analyzed on weeks 3, 7, and 9 using flow cytometry to detect CD45⁺/CD5⁺/CD19⁺ circulating MCL cells as previously described.¹⁶ Samples analyzed by flow cytometry for MCL cells, which were classified as live lymphocytes (live/CD45⁺), which coexpressed CD5 and CD19 (aberrant concurrent expression of these markers is found on human MCL cells). Mice were followed for survival, weighed every 2 to 3 days, and were euthanized if weight loss exceeded 20%. Left untreated, mice succumbed to disease within 9 to 10 weeks.

Tissue cross-reactivity

A GLP tissue cross-reactivity study on a full panel of normal human tissues was conducted at Charles River Laboratories, Frederick, MD. The tissue cross-reactivity study of the H90-5 Ab was performed with autopsy archival tissues from 3 healthy humans using the avidin-biotin immunoperoxidase method, as described previously.¹⁷ In total, 35 human organs were examined, and the primary Ab was H90-5 or human IgG1 κ used at concentrations of 2 $\mu\text{g}/\text{mL}$ and 10 $\mu\text{g}/\text{mL}$. Positive tissue staining was verified with an anti- β 2-microglobulin Ab. Specificity for the BAFF-R protein was examined with spot slides using recombinant human BAFF-R/TNFRSF13C Fc chimera protein (R&D Systems) as a positive control, and human parathyroid hormone-related protein (PTHrP)-1-34 (Sigma Chemical) as a negative control. Mononuclear cells in the human tonsil were selected as the ancillary control material because of the reported expression of BAFF-R in this tissue.¹⁸ Further details are provided in supplemental Methods.

Results

In vitro characterization of BAFF-R humanized Abs

As our goal is clinical application of this BAFF-R Ab, we elected to humanize our original chimeric Abs⁷ to reduce potential immunogenicity. Combination of the 3 VL and 3 VH humanized variants of

Table 1. Humanized C90 humanness score and binding affinity

Antibody	Humanness score VH/VL	K _D (nM)
C90	71/65	3.0
H90-1	86/86	4.0
H90-2	86/84	3.7
H90-3	86/85	5.0
H90-4	85/86	2.6
H90-5	85/84	3.6
H90-6	85/85	3.2
H90-7	82/86	3.8
H90-8	82/84	3.1
H90-9	82/85	3.4

BAFF-R chimeric C90 mAb (C90) resulted in 9 candidates with varying degrees of humanness (Table 1), with scores of ≥ 78 for VH and ≥ 84 for VL, supporting adequate humanness. All 9 variants (H90-1 through H90-9) were assessed for antigen binding, affinity, activity, and specificity in vitro, before identifying lead candidates for testing in mouse models.

Binding affinity was measured for each of the humanized Ab variants and compared with C90 using Biacore surface plasmon resonance imaging. Binding affinity for all variants were similar and essentially unchanged from C90 (Table 1). Similarly, all humanized variants bound recombinant BAFF-R protein-coated ELISA plates and had comparable dose response curves to the chimeric control (Figure 1A). The only suggestive differences were observed between Ab variants, and we elected to concentrate on H90-4 and H90-5, which both had high affinity (low K_D value) and relatively high humanness scores (VH ≥ 78 and VL ≥ 84 , respectively).

By flow cytometry analysis, H90-4 and H90-5 bound a panel of B-lymphoma cell lines, Raji (Burkitt's), Ly 10 (DLBCL), RL (FL), JeKo-1 and Z-138 (both MCL), MEC-1 (CLL), and RS4;11 (ALL) with no appreciable difference from the chimeric Ab, but did not bind BAFF-R-negative line HL-60 (acute myeloid leukemia) (Figure 1B).

Having previously established that the chimeric BAFF-R mAbs exert their effector function primarily via ADCC,⁷ we determined whether the humanized BAFF-R Abs induce ADCC against a panel of B-cell lymphoma cell lines (Figure 1C). Significant killing ($P < .01$), comparable with that observed with anti-CD20 mAb rituximab was observed for H90-4 and H90-5 in Ly 10, RL, JeKo-1, Z-138, Raji, and MEC-1. Notably, both H90-4 and H90-5 exhibited ADCC in RS4;11 whereas rituximab did not because this cell line lacks CD20. Having established activity against cell lines, we determined whether these 2 humanized candidates could bind (Figure 1D) and kill (Figure 1E) primary samples. Both H90-4 and H90-5 were equally effective at binding and mediating ADCC against 6 different primary samples from patients with B-cell tumors.

In addition, approximately 6% and 0.87% of humans carry the BAFF-R P21R (rs77874543) and G64V variant (rs547352394), respectively,¹⁹ making them 2 of the most significant variants of BAFF-R. We observed that H90-4 and H90-5 could bind both

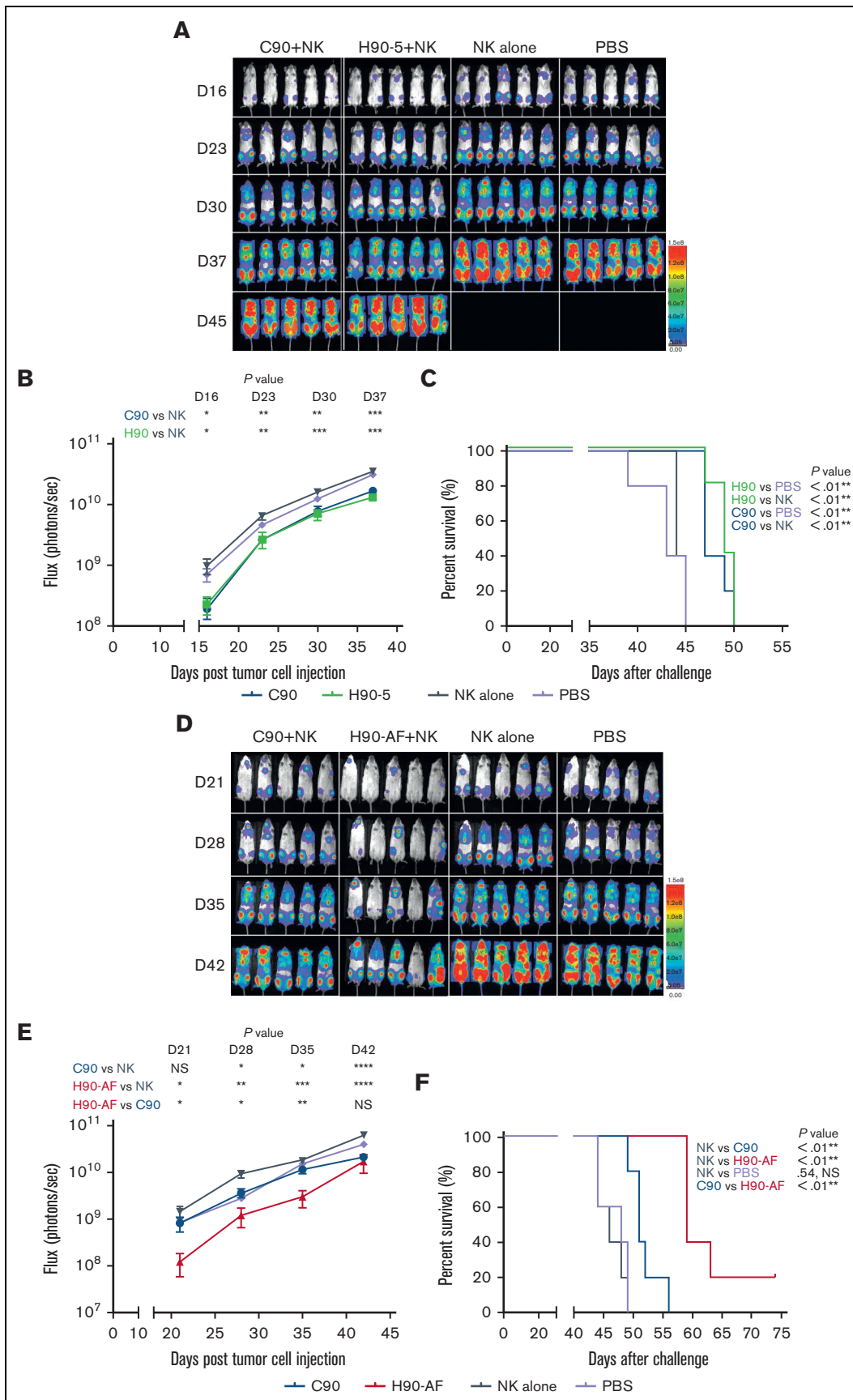


Figure 3.

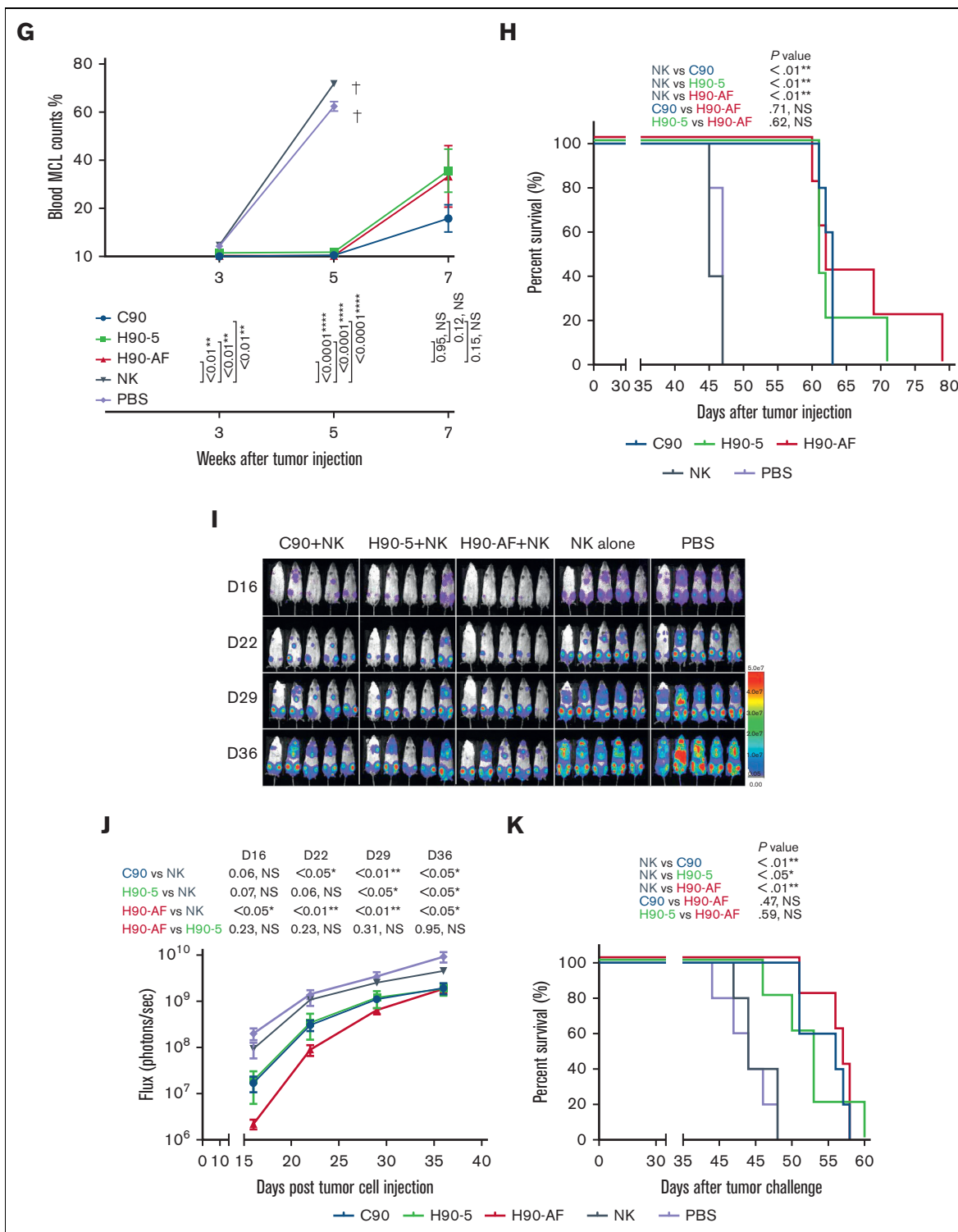


Figure 3 (continued) In vivo activity of humanized anti-BAFF-R mAbs. Z-138 MCL-luciferase cells (5×10^4) were injected IV into the tail veins of NSG mice on day 0. Mice were treated with 300 μ g Abs, as indicated, together with 15×10^6 Nk92 176V cells or 2×10^6 NK cells enriched from a healthy donor and 5×10^4 IU IL-2 on days 3, 7, 11, and 15. Tumor growth was monitored by bioluminescent imaging on the days indicated. (A) Tumor growth after treatment with either humanized BAFF-R Ab (H90-5), chimeric BAFF-R Ab (C90), or control treatments of NK cells alone or PBS only. (B) Flux (photons/s) was determined by measuring bioluminescence on day 16, 23, 30, and 37 after tumor cell injection. (C) Kaplan-Meier survival curves for each group of mice. (D) Z138 tumor growth after treatment with either C90, H90-AF, and control groups of NK alone or PBS only. (E) Flux was determined by measuring bioluminescence of luciferase on day 21, 28, 35 and 42 after tumor cell injection. (F) Kaplan-Meier survival curves for each group of mice. PDX MCL9606 (*BIRC3*^{L548fs}) cells (3×10^6) were inoculated via tail vein into 8-week-old NSG mice on day 0. Mice were treated with 300 μ g Abs (as indicated),

Table 2. Summary of cellular localization of H90-5 staining

Membrane and cytoplasmic elements	<ul style="list-style-type: none"> • Mononuclear cells in the colon (submucosal lymphoid aggregates), lymph node (follicles), prostate (small infiltrates), small intestine (submucosal lymphoid aggregates), spleen (white pulp), stomach (lamina propria), thymus (medulla), and tonsil (follicles)
Cytoplasmic elements	<ul style="list-style-type: none"> • Spindle cells in the bladder, cervix, esophagus, kidney, large intestine, liver, lung, mammary gland, ovary (stromal cells), pancreas, prostate, pituitary, small intestine, spleen, stomach, testis, ureter, and uterus (endometrial stromal cells) • Cells/processes associated with peripheral nerves in spinal nerve roots in the spinal cord • Intrinsic smooth myocytes in the bladder, cervix, and uterus (endometrium) • Striated (skeletal) myocytes in periocular skeletal muscle in the eye • Reticular cells in the lymph node and tonsil

variants P21R and G64V, similar to wild-type BAFF-R, whereas variant P21R was not recognized by commercial anti-BAFF-R mAb 11C1 (Figure 1F).

Generation and characterization of afucosylated humanized Abs

Glycoengineering, reducing fucosylation in the Fc domain, which generates greater ADCC through enhanced binding to FcγRIII receptor on immune effector cells, has successfully generated therapeutic Abs in clinical use.²⁰⁻²² N-linked oligosaccharides were cleaved from H90-5 as described in Methods. The resulting proportions of G0 and G1 core-fucosylated chains derived from H90-5 and H90-AF are shown in Figure 2. For H90-5, the G0F proportion accounts for about 75%, whereas the G0 portion is minor. In contrast, for H90-AF G0 becomes the predominant component (~75%), whereas the sum of G0F and G1F is less than 5% (Figure 2A). Deconvoluted mass spectra for H90-AF also revealed the extent of core glycosylated species, which correlate with the number of glucose residues and was consistent with successful afucosylation (Figure 2B; supplemental Table 2). Reducing fucosylation resulted in greater ADCC activity as demonstrated by in vitro ADCC assays comparing the activities of H90-5 and H90-AF with 4 human lymphoma/leukemia cell lines (Figure 2C-D). For example, the anti-CD20 Ab rituximab (positive control) induced ADCC against RL cells in a dose-dependent manner, with a 50% effective dose (EC₅₀) of 2.74 ng/mL and efficacy of ~80%. Under the same conditions, H9-5 showed only ~50% of the cell killing, with an EC₅₀ of 14.8 ng/mL. The ADCC activity of H90-AF was greatly enhanced, with an EC₅₀ of 0.26 ng/mL, and efficacy at 80%, comparable with that of rituximab. In addition, we confirmed the ability of H90-AF to mediate ADCC against Su-DHL-6, MEC-1 RL, Mino, Ramos, Z138, REC-1, Jeko-1, and Raji cells (supplemental Figure 1).

In vivo antitumor activity of humanized mAbs

Because there was no appreciable difference in the characteristics of H90-4 and H90-5, we selected H90-5 to develop for in vivo efficacy tests in mouse models. In vivo, we challenged NSG mice with a lethal IV dose of a stable red luciferase knock-in Z-138 MCL cell line followed by treatments with Ab (300 μg per mouse),

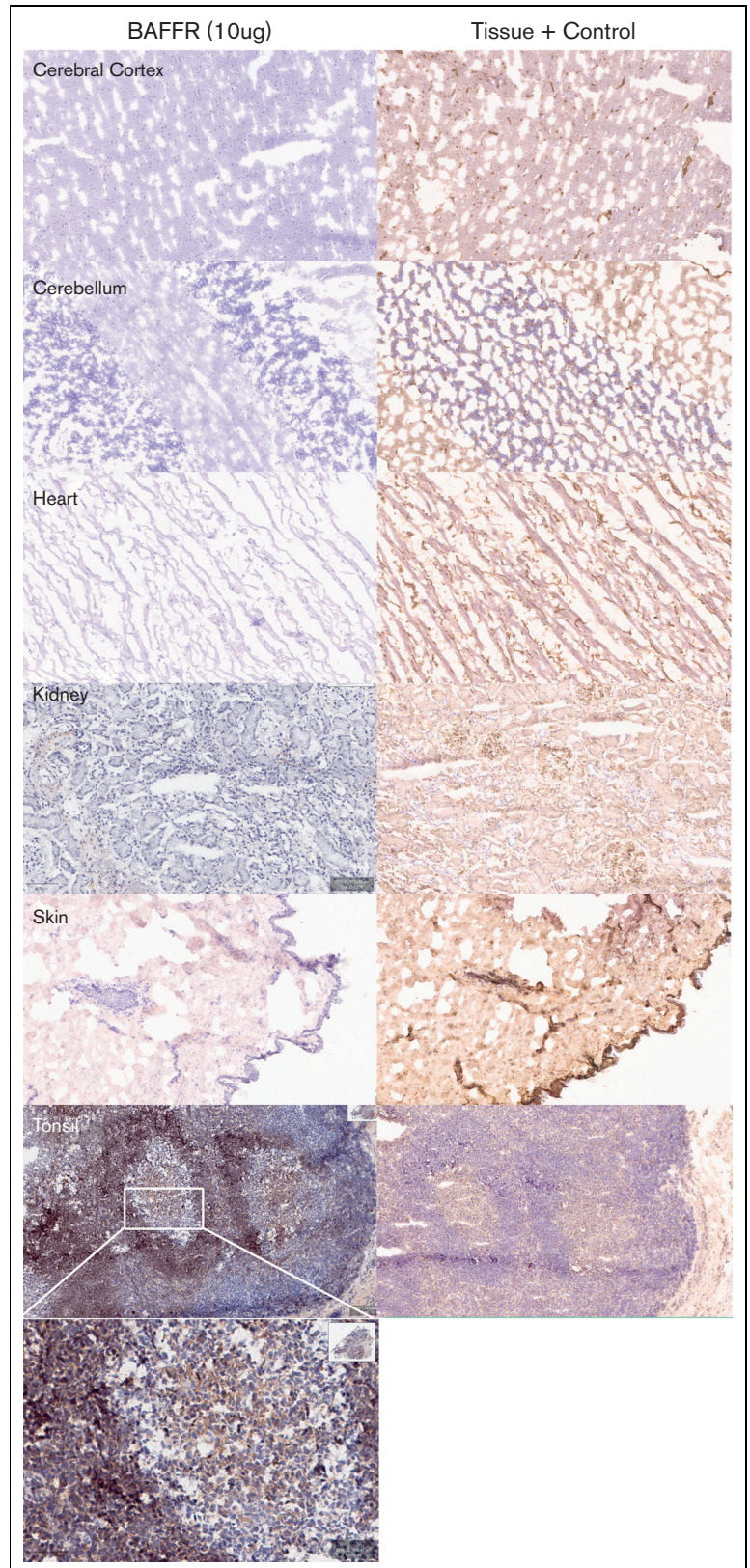
effector human NK cells, and IL-2, starting 3 days later (Figure 3A). Mice that had received humanized (H90) or chimeric (C90) BAFF-R Ab demonstrated significant retardation of tumor growth and significantly prolonged survival, compared with either control group, PBS or NK alone (Figure 3B-C). The humanized H90 showed similar anti-MCL tumor activity to the chimeric Ab. Similarly, H90-AF treatment in vivo was associated with significant anti-MCL activity under the same conditions (Figure 3D-F). Moreover, compared with C90, mice treated with afucosylated H90 showed prolonged survival. C90, H90-5, and H90-AF were also effective at suppressing tumor growth (Figure 3G) and prolonging survival (Figure 3H) in the MCL9606 (*BIRC3*^{L548fs}) PDX model of aggressive MCL compared with PBS or NK cells alone. We also investigated the activity of all 3 BAFF-R Abs in the Nalm6 xenograft model of ALL. All 3 Abs suppressed tumor growth (Figure 3I-J) and significantly extended survival (Figure 3K), compared with the NK cells alone control.

Tissue cross-reactivity

Next, we determined the potential cross-reactivity of H90-5 with normal human tissues using a full panel of cryosections. H90-5 produced weak to strong staining of the positive control material (recombinant human BAFF-R/TNFRSF13C Fc chimera UV-resin spot slides, designated rhBAFF-R) at the 2 concentrations tested (2 μg/mL and 10 μg/mL). H90-5 did not specifically react with the negative control material (human hypercalcemia of malignancy peptide, amino acid residues 1-34, UV-resin spot slides, designated PTHrP 1-34) at either staining concentration. There also was no staining of the assay control slides. Mononuclear cells in the human tonsil was selected as the ancillary positive control because of the known expression of BAFF-R in lymphoid cells,¹⁸ and, indeed, H90-5 stained the membrane and cytoplasm of mononuclear cells observed primarily within the mantle cuffs of follicles in the human tonsil with varying intensities at concentrations ranging from 2 to 10 μg/mL (Table 2; Figure 4). The panel of human tissues showed occasional cytoplasmic staining with H90-5, but no tissue showed similar membrane staining with H90-5, except for expected staining of other lymphoid tissues. Binding to cytoplasmic sites is generally considered of little to no toxicologic significance because of the limited ability of Ab-based therapeutics to

Figure 3 (continued) IL-2, and NK cells, as described earlier for panel D, on days 3, 7, 11, and 15. Control groups received the same volume of injection with NK cells alone or PBS. (G) Flow cytometry for CD45⁺/CD5⁺/CD19⁺ cells representing MCL at the indicated times after tumor inoculation. Mice in the PBS and NK cells only control groups were all euthanized before week 7 because weight loss exceeded 20%, indicated by †. (H) Kaplan-Meier survival curves for each group of mice. Nalm6 ALL-luciferase cells (1 × 10⁵) were injected IV into the tail veins of NSG mice on day 0. Mice were treated with 300 μg Abs, as indicated, together with 1.5 × 10⁶ NK cells enriched from a healthy donor and 5 × 10⁴ IU IL-2 on days 3, 7, 11, and 15. Tumor growth was monitored by bioluminescent imaging on the days indicated. (I) Tumor growth after treatment with either chimeric BAFF-R Ab (C90), humanized BAFF-R Ab (H90-5), afucosylated H90-5 (H90-AF), or control treatments of NK cells alone or PBS only. (J) Flux was determined by measuring bioluminescence of luciferase on days 16, 22, 29 and 36 after tumor cell injection. (K) Kaplan-Meier survival curves for each group of mice. **log-rank *P* values.

Figure 4. Tissue specificity of BAFF-R H90-5 by immunohistochemistry. Frozen tissue sections were stained at a concentration of 10 $\mu\text{g}/\text{mL}$ with BAFF-R H90 (top row) using various normal human tissue sections from 3 separate donors. Anti- β -2-microglobulin (bottom row) was used as an internal tissue control. Lymphoid tissues such as the tonsil (positive control) showed distinct, strong staining within the mantle cuffs of the follicles. No nonlymphoid frozen tissues showed cross-reactivity with BAFF-R H90-5. Representative tissue sections are shown (original magnification $\times 40$; except for tonsil shown at original magnifications $\times 40$ and $\times 200$).



access the cytoplasmic compartment *in vivo*.²³ The comprehensive list of all tissues tested is shown in supplemental Table 1.

Discussion

BAFF-R is an appealing target for immunotherapy because it is a B-cell lineage surface marker highly expressed by various mature B-cell malignancies.⁵ We predict that the capacity of clonal B-cell tumors to escape anti-BAFF-R therapy by downregulation of antigen expression would also be limited, because BAFF-R signaling is a driver of B-cell growth and survival via activation of NF- κ B pathways.^{3,18,24-28} Furthermore, increased BAFF-R expression is correlated with disease progression in patients with B-cell lymphoma and pre-B ALL²⁹⁻³¹; whereas expression is undetected on pre-B-cells,¹⁸ making B-cell aplasia an unlikely outcome of BAFF-R-directed therapies.

In an extensive survey of mAbs in successful clinical use, Hwang et al documented a higher incidence of anti-Ab responses (AAR) for chimeric mAbs than for humanized mAbs.¹⁴ Anti-Ab responses limit the clinical utility of mAbs through a combination of rapid elimination of the therapeutic mAb and infusion reaction toxicity. In this report we have described the generation of a specific humanized anti-BAFF-R mAb, which retain the *in vitro* and *in vivo* antitumor activity profiles of a previously described chimeric BAFF-R mAb (C90) from which it was derived.⁷

Nine different humanized variants were created from 3 humanized VH and 3 humanized VL sequences and initially tested for binding affinity to recombinant BAFF-R. Surprisingly, binding affinities of all of these humanized BAFF-R Abs were similar, as K_D values ranged from 2.6 to 5.0 nM and were comparable with the K_D of the parental chimeric BAFF-R Ab (3.0 nM) (Table 1). We elected to focus on H90-4 and H90-5, which both had high affinity and relatively high humanness scores (VH \geq 78 and VL \geq 84, respectively).

The specificity of these humanized BAFF-R mAbs was demonstrated by flow cytometry analysis of a variety of B-cell malignancy cell lines, and in 6 primary samples from patients with MCL or marginal zone lymphoma (MZL) (Figure 1B). In addition, immunohistochemical analysis of H90-5 against a panel of normal human tissues showed the expected pattern of staining; membrane and cytoplasmic staining in mononuclear cells in several human tissues, consistent with the reported expression of its target protein, BAFF-R, by B cells^{18,32} but not in any other tissue type (Figure 4).

We showed that the humanized BAFF-R mAb H90-5 was as effective at delaying tumor growth and prolonging survival as the parent chimeric mAb C90 in 2 separate *in vivo* xenograft models of human lymphoma and 1 model of human leukemia, including 1 MCL PDX (Figure 3A-K). Our prior study showed that parental, chimeric C90 BAFF-R Abs mediated antitumor effects through multiple potential mechanisms of action, including inhibition of BAFF ligand binding to BAFF-R on tumor cells in a dose-dependent manner.⁷ However, the primary mechanism of action was likely ADCC, which suggested a strategy for further optimization. Indeed, afucosylated BAFF-R Ab, H90-AF, demonstrated superior ADCC compared with the parental humanized Ab *in vitro* (Figure 2C-D), and was at least as effective in both *in vivo* models tested (Figure 3G-K). Taken together, these data suggest that afucosylated H90-5 is a suitable lead candidate for further clinical development.

To our knowledge, the only other anti-BAFF-R therapeutic mAb is the fully human B-1239/VAY736 that has been investigated in ALL and CLL.⁹⁻¹¹ Similar to H90-5 and H90-AF, B-1239/VAY736 has been shown to kill CLL primarily by ADCC.¹⁰ B-129/VAY736 demonstrated *in vivo* activity preclinically in the E μ -TCL CLL model in SCID mice in combination with ibrutinib,¹¹ and B-129/VAY736 has entered early clinical testing, as ivalumab, in combination with ibrutinib in CLL. Results of this phase 1b trial were recently reported, showing favorable safety, tolerability, and preliminary efficacy, suggesting the therapeutic potential of BAFF-R mAbs in B-cell malignancies.¹³

Finally, these humanized BAFF-R immunoglobulin gene sequences can be incorporated into emerging chimeric antigen receptor,^{33,34} dual chimeric antigen receptor in combination with CD19,³⁵ and bispecific T-cell engager platforms to generate novel therapeutic agents with different mechanisms of action against B-cell malignancies.

Acknowledgments

Research reported in this article included work performed in the Analytical Cytometry Core and Small Animal Imaging Core supported by the National Cancer Institute (NCI) of the National Institutes of Health (NIH) under award number P30CA033572. The content is solely the responsibility of the authors and does not necessarily represent the official views of the NIH. The authors are grateful for the support from the Toni Stephenson Lymphoma Center at the Beckman Research Institute of City of Hope. The study was also supported by the Leukemia and Lymphoma Society: Translational Research Program (TRP 6540-18; primary investigator (PI), L.W.K.), Mantle Cell Lymphoma Research Initiative (MCL 7000-18; PI, L.W.K.); the NIH/NCI (SPORE 2P50CA107399; PIs, S.J.F. and L.W.K.; 1R21CA223141; PI, H.Q.).

Authorship

Contribution: Z.D., E.T., A.A., W.A.C., B.Z.K., V.L., T.Z., Z.W., S.S., W.N., X.Z., F.H., and E.O. contributed experimental data; D.L.S. contributed to data analysis and manuscript preparation; J.Y.S., S.C., A.V.D., J.Z., and Q.Z. conducted data analysis; L.W.K. oversaw the project including data analysis and manuscript writing; and H.Q. designed and initiated the project, oversaw experiments, and analyzed the data.

Conflict-of-interest disclosure: L.W.K. and H.Q. report consultancy for, and equity ownership in Innolife and Pepromene Bio, Inc. J.Z. has equity ownership and is an employee of Innolife. X.Z., W.N., F.H., and Q.Z. are employees of Shanghai Escugen Biotechnology Co Ltd. The remaining authors declare no competing financial interests.

ORCID profiles: J.Y.S., 0000-0003-3497-2513; E.T., 0000-0002-6012-1117; W.A.C., 0000-0001-9131-8556; B.Z.K., 0000-0002-0944-0753; D.L.S., 0000-0003-2400-659X; Q.Z., 0000-0003-1158-0357; H.Q., 0000-0003-4686-929X; L.W.K., 0000-0002-1884-5349.

Correspondence: Larry W. Kwak, Translational Research & Developmental Therapeutics; Toni Stephenson, Lymphoma Center; Michael Friedman, Beckman Research Institute of City of Hope, 1500 East Duarte Rd, Duarte, CA 91010; email: lkwak@coh.org.

References

1. Cuesta-Mateos C, Alcaraz-Serna A, Somovilla-Crespo B, Munoz-Calleja C. Monoclonal antibody therapies for hematological malignancies: not just Q23 lineage-specific targets. *Frontiers in Immunology*. 2018;8:1936.
2. Ma Y, Zhang P, Gao Y, Fan H, Zhang M, Wu J. Evaluation of AKT phosphorylation and PTEN loss and their correlation with the resistance of rituximab in DLBCL. *Int J Clin Exp Pathol*. 2015;8(11):14875-14884.
3. Hildebrand JM, Luo Z, Manske MK, et al. A BAFF-R mutation associated with non-Hodgkin lymphoma alters TRAF recruitment and reveals new insights into BAFF-R signaling. *J Exp Med*. 2010;207(12):2569-2579.
4. Thompson JS, Bixler SA, Qian F, et al. BAFF-R, a newly identified TNF receptor that specifically interacts with BAFF. *Science*. 2001;293(5537):2108-2111.
5. Novak AJ, Grote DM, Stenson M, et al. Expression of BlyS and its receptors in B-cell non-Hodgkin lymphoma: correlation with disease activity and patient outcome. *Blood*. 2004;104(8):2247-2253.
6. Furie R, Petri M, Zamani O, et al. A phase III, randomized, placebo-controlled study of belimumab, a monoclonal antibody that inhibits B lymphocyte stimulator, in patients with systemic lupus erythematosus. *Arthritis Rheum*. 2011;63(12):3918-3930.
7. Qin H, Wei G, Sakamaki I, et al. Novel BAFF-receptor antibody to natively folded recombinant protein eliminates drug-resistant human B-cell malignancies In Vivo. *Clin Cancer Res*. 2018;24(5):1114-1123.
8. Lee CV, Hymowitz SG, Wallweber HJ, et al. Synthetic anti-BR3 antibodies that mimic BAFF binding and target both human and murine B cells. *Blood*. 2006;108(9):3103-3111.
9. Parameswaran R, Lim M, Fei F, et al. Effector-mediated eradication of precursor B acute lymphoblastic leukemia with a novel Fc-engineered monoclonal antibody targeting the BAFF-R. *Mol Cancer Therapeut*. 2014;13(6):1567-1577.
10. McWilliams EM, Cheney C, Jones JA, et al. B-1239, a novel anti-BAFF-R afucosylated human antibody, promotes potent natural killer cell-mediated antibody dependent cellular cytotoxicity in chronic lymphocytic leukemia cells in-vitro and depletion of circulating leukemic CLL B cells in-vivo. *Blood*. 2013;122(21):4185.
11. McWilliams EM, Lucas CR, Chen T, et al. Anti-BAFF-R antibody VAY-736 demonstrates promising preclinical activity in CLL and enhances effectiveness of ibrutinib. *Blood Adv*. 2019;3(3):447-460.
12. Rogers KA, Flinn IW, McGarry C, et al. Phase Ib study of ionalumab (VAY736) and ibrutinib in patients with chronic lymphocytic leukemia (CLL) on ibrutinib therapy. *Blood*. 2020;136(Supplement 1):13-14.
13. Rogers KA, Flinn IW, Stephens DM, et al. Investigating the addition of ionalumab (VAY736) to ibrutinib in patients with chronic lymphocytic leukemia (CLL) on ibrutinib therapy: results from a phase Ib study. 2021;138(Supplement 1):2631.
14. Hwang WY, Foote J. Immunogenicity of engineered antibodies. *Methods*. 2005;36(1):3-10.
15. Townsend EC, Murakami MA, Christodoulou A, et al. The public repository of xenografts enables discovery and randomized phase II-like trials in mice. *Cancer Cell*. 2016;29(4):574-586.
16. Thieme E, Liu T, Bruss N, et al. Dual BTK/SYK inhibition with CG-806 (luxetpinib) disrupts B-cell receptor and Bcl-2 signaling networks in mantle cell lymphoma. *Cell Death Dis*. 2022;13(3):246.
17. Lin Q, Price SA, Skinner JT, et al. Systemic evaluation and localization of resistin expression in normal human tissues by a newly developed monoclonal antibody. *PLoS One*. 2020;15(7):e0235546.
18. Rodig SJ, Shahsafaei A, Li B, Mackay CR, Dorfman DM. BAFF-R, the major B cell-activating factor receptor, is expressed on most mature B cells and B-cell lymphoproliferative disorders. *Hum Pathol*. 2005;36(10):1113-1119.
19. Block V, Sevdali E, Recher M, et al. COVID-associated B cell activating factor receptor variants change receptor oligomerization, ligand binding and Q27 signaling responses. *J Clin Immunol*. 2022:1-15.
20. Shields RL, Lai J, Keck R, et al. Lack of fucose on human IgG1 N-linked oligosaccharide improves binding to human Fcγ3 and antibody-dependent cellular toxicity. *J Biol Chem*. 2002;277(30):26733-26740.
21. Shinkawa T, Nakamura K, Yamane N, et al. The absence of fucose but not the presence of galactose or bisecting N-acetylglucosamine of human IgG1 complex-type oligosaccharides shows the critical role of enhancing antibody-dependent cellular cytotoxicity. *J Biol Chem*. 2003;278(5):3466-3473.
22. Niwa R, Sakurada M, Kobayashi Y, et al. Enhanced natural killer cell binding and activation by low-fucose IgG1 antibody results in potent antibody-dependent cellular cytotoxicity induction at lower antigen density. *Clin Cancer Res*. 2005;11(6):2327-2336.
23. Leach MW, Halpern WG, Johnson CW, et al. Use of tissue cross-reactivity studies in the development of antibody-based biopharmaceuticals: history, experience, methodology, and future directions. *Toxicol Pathol*. 2010;38(7):1138-1166.
24. Fu L, Lin-Lee YC, Pham LV, Tamayo AT, Yoshimura LC, Ford RJ. BAFF-R promotes cell proliferation and survival through interaction with IKKβ and NF-κB/c-Rel in the nucleus of normal and neoplastic B-lymphoid cells. *Blood*. 2009;113(19):4627-4636.
25. Nakamura N, Hase H, Sakurai D, et al. Expression of BAFF-R (BR 3) in normal and neoplastic lymphoid tissues characterized with a newly developed monoclonal antibody. *Virchows Arch*. 2005;447(1):53-60.
26. Paterson JC, Tedoldi S, Craxton A, et al. The differential expression of LCK and BAFF-receptor and their role in apoptosis in human lymphomas. *Haematologica*. 2006;91(6):772-780.

27. Pham LV, Fu L, Tamayo AT, et al. Constitutive BR3 receptor signaling in diffuse, large B-cell lymphomas stabilizes nuclear factor-kappaB-inducing kinase while activating both canonical and alternative nuclear factor-kappaB pathways. *Blood*. 2011;117(1):200-210.
28. Liu M, Song W, Zhang J, Sun M, Sun X, Yu Q. Non-canonical NF-kappaB Plays a Pivotal Role in Non-Hodgkin's Lymphoma. *Cell Biochem Biophys*. 2015;72(3):681-685.
29. Li YJ, Jiang WQ, Rao HL, et al. Expression of BAFF and BAFF-R in follicular lymphoma: correlation with clinicopathologic characteristics and survival outcomes. *PLoS One*. 2012;7(12):e50936.
30. Shen X, Wang M, Guo Y, Ju S. The correlation between non-Hodgkin lymphoma and expression levels of B-cell activating factor and its receptors. *Adv Clin Exp Med*. 2016;25(5):837-844.
31. Parameswaran R, Muschen M, Kim YM, Groffen J, Heisterkamp N. A functional receptor for B-cell-activating factor is expressed on human acute lymphoblastic leukemias. *Cancer Res*. 2010;70(11):4346-4356.
32. Ng LG, Sutherland AP, Newton R, et al. B cell-activating factor belonging to the TNF family (BAFF)-R is the principal BAFF receptor facilitating BAFF costimulation of circulating T and B cells. *J Immunol*. 2004;173(2):807-817.
33. Dong Z, Cheng WA, Smith DL, et al. Antitumor efficacy of BAFF-R targeting CAR T cells manufactured under clinic-ready conditions. *Cancer Immunol Immunother*. 2020;69(10):2139-2145.
34. Qin H, Dong Z, Wang X, et al. CAR T cells targeting BAFF-R can overcome CD19 antigen loss in B cell malignancies. *Sci Transl Med*. 2019;11(511):eaaw9414.
35. Wang X, Dong Z, Awuah D, et al. CD19/BAFF-R dual-targeted CAR T cells for the treatment of mixed antigen-negative variants of acute lymphoblastic leukemia. *Leukemia*. 2022;36(4):1015-1024.